energies

MDPI

Article

Optimal Evolutionary Dispatch for Integrated Community Energy Systems Considering Uncertainties of Renewable Energy Sources and Internal Loads

Xinghua Liu [1], Shenghan Xie [1], Chen Geng [1], Jianning Yin [1,*], Gaoxi Xiao [2] and Hui Cao [3]

[1] School of Electrical Engineering, Xi'an University of Technology, Xi'an 710048, China; liuxh@xaut.edu.cn (X.L.); xiesh122@163.com (S.X.); gengchen@stu.xaut.edu.cn (C.G.)
[2] School of Electrical and Electronic Engineering, Nanyang Technological University, Singapore 639798, Singapore; egxxiao@ntu.edu.sg
[3] School of Electrical Engineering, Xi'an Jiaotong University, Xi'an 710049, China; huicao@mail.xjtu.edu.cn
* Correspondence: yinjianning@xaut.edu.cn

Abstract: For the future development of integrated energy systems with high penetration of renewable energy, an integrated community energy systems (ICES) dispatch model is proposed including various renewable energy sources and energy conversion units. Energy coupling matrices of ICES based on traditional energy hub (EH) models are constructed. Uncertainties of long-term forecast data of renewable energy sources and internal loads are depicted by multi-interval uncertainty sets (MIUS). To cope with the impacts caused by uncertainties of renewable energy sources and internal loads, the whole dispatch process is divided into two stages. Considering various constraints of ICES, we solved the dispatch model through the improved particle swarm optimization (IPSO) algorithm in the first stage. The optimal evolutionary dispatch is then proposed in the second stage to overcome the evolution and errors of short-term forecast data and obtain the optimal dispatch plan. The effectiveness of the proposed dispatch method is demonstrated using an example considering dramatic uncertainties. Compared with the traditional methods, the proposed dispatch method effectively reduces system operating costs and improves the environmental benefits, which helps to achieve a win-win situation for both energy companies and users.

Keywords: integrated community energy system; energy hub; renewable energy source; optimal dispatch

Citation: Liu, X.; Xie, S.; Geng, C.; Yin, J.; Xiao, G.; Cao, H. Optimal Evolutionary Dispatch for Integrated Community Energy Systems Considering Uncertainties of Renewable Energy Sources and Internal Loads. *Energies* **2021**, *14*, 3644. https://doi.org/10.3390/en14123644

Academic Editor: Albert Smalcerz

Received: 14 May 2021
Accepted: 14 June 2021
Published: 18 June 2021

1. Introduction

The gradual scarcity of fossil energy reserves and the increasingly serious environmental pollution have forced people to reform the existing energy consumption patterns; integrated energy systems (IES) are the important technical support for this reform [1–5]. As an important member of various types of IES, integrated community energy systems (ICES) have a bright prospect with their complete functions and easy implementation. To achieve energy saving and emission reduction, various kinds of renewable energy sources have been absorbed in ICES. However, there is a large amount of abandoned energy in ICES caused by randomness and volatility of renewable energy sources [6–8]. If the abandoned energy can be utilized through proper dispatching, the economic and environmental benefits of ICES could be significantly improved. Applying the functions of ICES flexibly to effectively improve energy efficiency and promote the consumption of renewable energy has attracted attention recently.

In order to avoid the energy abandonment, the techniques for forecasting renewable energy such as wind energy and solar energy has developed greatly in recent years [9]. In

[10], a short-term forecast method based on cuckoo search and differential evolution algorithms was proposed. In [11], the authors provided the method for long-term forecasting of intermittent wind and photovoltaic resources, which depended on an adaptive neuro fuzzy inference system. Although the current forecasting technology for wind turbines (WTs) and photovoltaic units (PVs) has made great progress, certain deviations still exist in the forecast accuracy. These deviations become uncertain factors of the scheduling process.

Several recent scientific studies on power grids focus on handling the uncertainty of parameters. The authors of [12,13] show that robust optimization based on cardinality set or stochastic optimization is a viable technique to deal with uncertainty of parameters. However, the uncertainty of ICES is more complicated than that of the grid system. Uncertainty modeling alone cannot be used to improve the operation effect. An overall dispatching strategy needs to be proposed to improve the renewable energy consumption capacity of ICES.

ICES can combine various kinds of energies in a certain region, which is the key to solving energy abandonment and improving system performance. In [14,15], the authors studied the operation plans that transfer abandoned wind and solar energy to electric boilers for heating. In [16], hydrogen energy storage technology is employed to convert redundant wind and solar power. These references illustrate the role of energy coupling and energy storage in absorbing renewable energy output. However, using electric–thermal coupling equipment as the consumptive channel of energy is restricted by seasons and regions. Hence, these kinds of schemes have no universal applicability. Hydrogen storage technology is still immature and cannot be used on the large scale in the short term.

Different kinds of optimization methods are also helpful in improving the renewable energy consumption. The authors of [17,18] used robust optimization to obtain a day-ahead scheduling scheme, which is robust under the wind and solar power uncertainties and takes into account the system safety as well. However, schemes by robust optimization are too conservative for operation and tend to sacrifice some economic benefits.

Power to gas (P2G) is a kind of technology that converts electric energy into methane through the chemical reaction of water electrolysis and methanation, which deepens the coupling between the power system and the natural gas network in the ICES [19,20]. P2G units can transform redundant electric energy to natural gas P2G units and cooperate with gas storage equipment to store the converted energy. This process can effectively absorb the redundant electricity generated by WTs and PVs in the ICES [21]. As natural gas is easier to store than electric energy, P2G units have a good application prospect in ICES. P2G units are selected as an important part in the ICES model of our work.

Considering preview problems, we propose a dispatch process to optimize the operation of ICES to fully absorb the WTs' and PVs' output under the uncertainties of renewable energy sources and internal loads. An energy hub (EH) model of ICES including P2G units is built to provide operational flexibility and improve economic performance. To decrease the conservatism of dispatch results, a strategy that can dynamically adjust the operation plan according to the short-term forecast is introduced to consume renewable power as much as possible. The detailed contributions of this article are as follows:

- Multi-interval uncertainty sets (MIUS) for the forecast data of renewable energy sources and internal loads are introduced. Multiple forecast scenarios are generated in the day-ahead dispatch stage through MIUS and generate a day-ahead scheduling plan for each forecast scenario. They fully consider the uncertainty of the forecast data and ensure a sufficient time for the actual dispatch work.
- Considering that the short-term forecasting data (SFD) will continue to evolve, optimal evolutionary dispatch plan (OEDP) is proposed. OEDP will make timely adjustments according to the evolution of SFD to make the dispatch plan performance better.

- Real-time Adjusting Strategy (RAS) is proposed to solve the impact which caused by the deviation between SFD and the actual situation of dispatch process. It further improves the utilization rate of renewable energy and ensures the safety of users' energy demand.

The rest of this paper is organized as follows. Section 2 describes the details of models and methods we designed. In Section 3, the simulation results of the dispatch process and examples for comparison is exhibited, superiority of the dispatch process is discussed and validated in this section. Finally, Section 4 concludes the paper.

2. Models and Methods

In this section, the details of proposed methodology including energy hub (EH) models for ICES, multi-interval uncertainty sets (MIUS) for day-ahead long-term forecast data (DLFD), improved particle swarm optimization (IPSO) algorithm for optimal deterministic dispatch and optimal evolutionary dispatch are elaborated. Figure 1 demonstrates the framework of the proposed methodology. The description of all types of parameter symbols and their units are listed in Table 1.

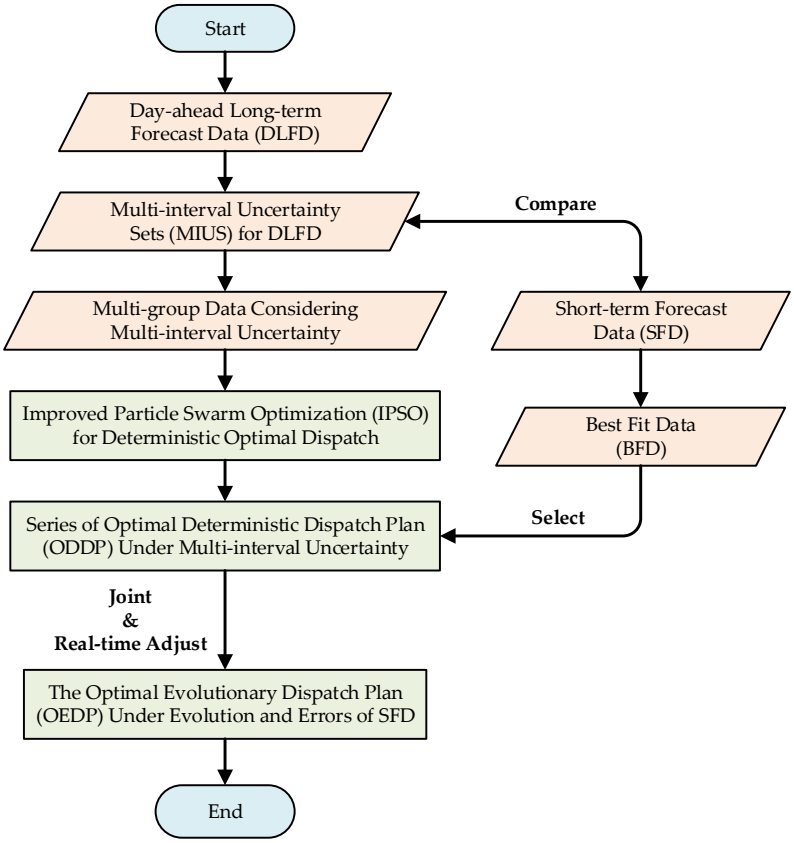

Figure 1. The framework of optimal evolutionary dispatch for integrated community energy systems.

Table 1. Description of all types of parameter symbols.

Parameter [1]	Description (Units)
$P^{x}_{x,x}$ $P^{x}_{x,x}$	Electric power (MW)
$Q^{x}_{x,x}$	Cooling/Heating power (MW)
$V^{x}_{x,x}$	Gas volume (m^3)

$C^{x}_{x,x}$	Cost (USD)
$c^{x}_{x,x}$	Energy price (USD)

[1] This table lists all the types of parameter symbols used in this article. The upper and lower corners of the symbol are not fixed and "x" is determined according to the specific meaning of the symbol.

2.1. Energy Hub (EH) Models for Integrated Community Energy Systems (ICES)

The EH model is used to establish ICES, which is a model that can illustrate the conversion, distribution and storage of multiple energy sources [22–24]. The EH model consumes energy at its entrance and provides necessary energy services at its output side. Inside the EH model, energy is converted into different forms through coupling devices [25–27]. The EH model topology is exhibited in Figure 2a.

Various energy coupling devices are applied in the ICES model of this paper to allow flexible conversion of various energies. The ICES consists of an electrical power system, natural gas system, district heating system, and multi-energy loads. The diagram of the ICES investigated in this article is given in Figure 2b. Units marked by "#" in Figure 2b are only enabled in the optimal evolutionary dispatch, and units without any marks are enabled in both day-ahead deterministic dispatch and optimal evolutionary dispatch. The energy storage system, such as battery and gas tank, can be equipped to improve the reliability and economy of the system [28,29].

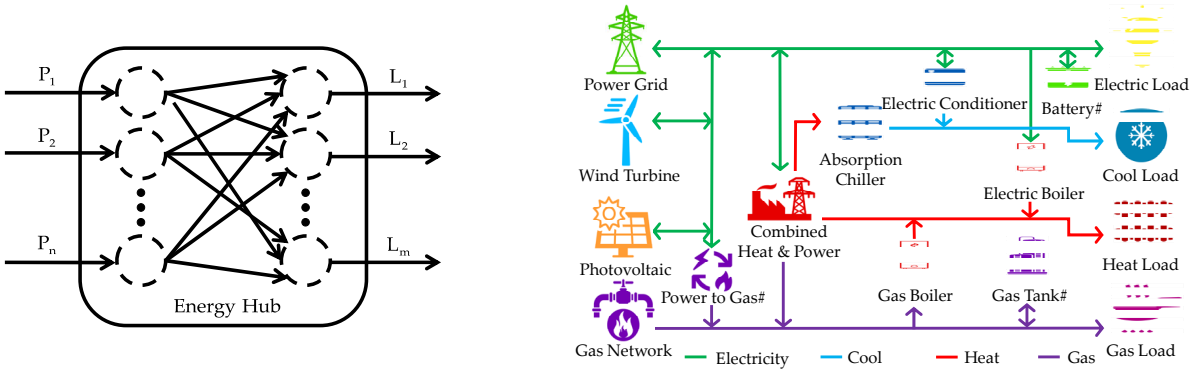

(**a**) (**b**)

Figure 2. Diagrams of EH models: (**a**) the topology diagram of EH models; (**b**) the schematic diagram of the EH model for ICES which is established in this paper.

The energy conversion relationship in the IES model can be described as follows:

$$\begin{bmatrix} P_{L,e} \\ Q_{L,c} \\ Q_{L,h} \\ V_{L,g} \end{bmatrix} = \begin{bmatrix} 1-v_{EC}-v_{EB} & \eta_{CHP,e} & 1 & 1 \\ u_2 v_{EC} COP_{EC} & u_2 \eta_{CHP,h} COP_{AC} & 0 & 0 \\ u_1 v_{EB} \eta_{EB,h} & u_1(\eta_{CHP,h}+\eta_{GB,h}) & 0 & 0 \\ 0 & 1-v_{CHP}-v_{GB} & 0 & 0 \end{bmatrix} \begin{bmatrix} P_{buy,e} \\ V_{buy,g} \\ P_{W,e} \\ P_{S,e} \end{bmatrix}, \quad (1)$$

where $P_{L,e}$, $Q_{L,c}$, $Q_{L,h}$ and $V_{L,g}$ represent the electric load (EL), cooling load, heating load (HL) and gas load (GL) in the model, respectively; $P_{buy,e}$, $V_{buy,g}$, $P_{W,e}$ and $P_{S,e}$ represent the power purchased from the grid, the gas purchased from the gas network, the power generated by WTs and PVs, respectively; v_{EC}, v_{EB}, v_{CHP} and v_{GB} are the distribution coefficients of electric conditioner, electric boiler (EB), combined heat and power unit (CHP) and gas boiler (GB), respectively; $\eta_{CHP,h}$ is the waste heat recovery

coefficient of CHP; $\eta_{EB,h}$ and $\eta_{GB,h}$ are the heating coefficient of EB and GB, respectively; COP_{EC} and COP_{AC} are the refrigeration coefficients of EC and absorption chiller, respectively; u_1 and u_2 are the binary variable representing the season, $u_1 + u_2 = 1 \& u_1, u_2 \in \{0,1\}$.

2.2. Multi-Interval Uncertainty Sets (MIUS) for Day-Ahead Long-Term Forecast Data (DLFD)

Though the current forecasting technology is advanced, there are still many uncertainties. We need to build uncertainty sets to describe uncertainties [17,18]. In the dispatch problem of energy systems, the commonly used uncertainty set for modeling the uncertainties in renewable energy and load is as follows [30,31]:

$$\mathbf{U} = \left\{ u^t : -\Delta u^t \leqslant u^t - \tilde{\bar{u}}^t \leqslant \Delta u^t, \sum_{t \in \mathbf{T}} \left| u^t - \tilde{\bar{u}}^t \right| / \Delta u^t \leqslant \Gamma \right\}, \quad (2)$$

where u^t is the uncertainty parameter, Δu^t is the deviation of u^t, $\tilde{\bar{u}}^t$ is the nominal value of u^t, and Γ is the budget of uncertainty.

Equation (2) describes a single-interval uncertainty set (SIUS), which defines the value of u^t on a single interval. The SIUS needs no probability information about the forecast error, while it results in strong conservatism. Inputting uncertainty data with strong conservatism into the dispatch strategy will result in poor performance to the final output dispatch plan. In order to embed more information into the uncertainty set to reduce the conservatism, the uncertainty sets are divided into multi-interval to construct a MIUS [32], as follows:

$$\mathbf{U} = \left\{ u^t : u^t = \tilde{u}^t \cdot \left(1 + v_u^t\right), \underline{v}_u^{k,t} \varepsilon^{k,t} \leqslant v_u^t \leqslant \bar{v}_u^{k,t} \varepsilon^{k,t}, \varepsilon^{k,t} \in \{0,1\}, \sum_{k \in K} \varepsilon^{k,t} = 1, \sum_{t \in T} \varepsilon^{k,t} = \Gamma^k \right\}, \quad (3)$$

where v_u^t is the deviation ratio of u^t, $\underline{v}_u^{k,t}$ and $\bar{v}_u^{k,t}$ are the lower bound and upper bound of the interval k of v_u^t, respectively, $\varepsilon^{k,t}$ is binary variable to indicate whether v_u^t is located in the interval k. Γ^k is the budget of the interval k, and k is the index of each interval. Based on the assumption that the deviation ratio v_u^t is independent and identically distributed, the budget Γ^k can be calculated by

$$\Gamma^k = N_d \int_{\underline{v}_u^k}^{\bar{v}_u^k} f(v_u) dv_u, \quad (4)$$

where $f(v_u)$ is the probability density function of v_u^t.

Compared with the SIUS, the MIUS embeds more distribution information of the uncertainties and the dispatch results can be less conservative. In this paper, the DLFD is brought into the MIUS model to obtain the multi-group data considering multi-interval uncertainties. The specific process of this step is shown as Figure 3a.

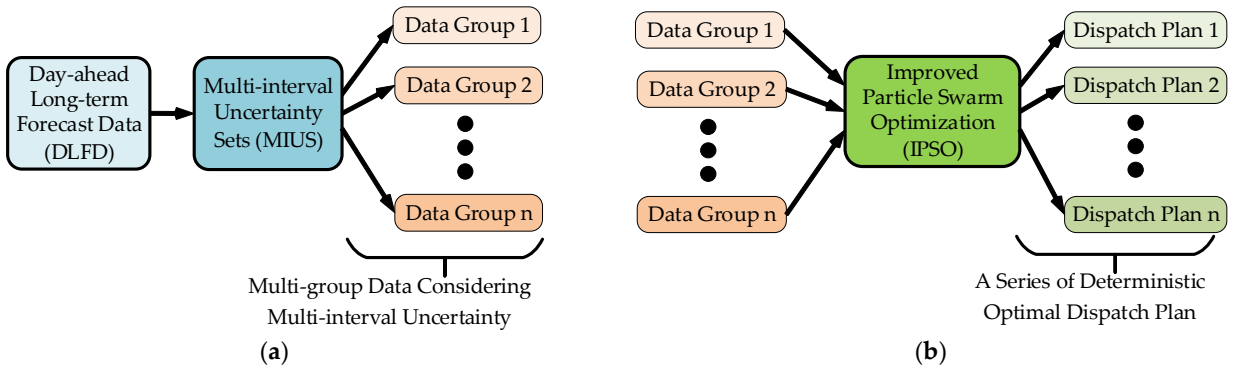

Figure 3. Process diagrams of method to obtain the multi-group data and a series of ODDP: (**a**) process to obtain the multi-group data; (**b**) process to obtain a series of ODDP.

2.3. Improved Particle Swarm Optimization (IPSO) for Optimal Deterministic Dispatch

Before the optimal evolutionary dispatch, the day-ahead optimal deterministic dispatch plan (ODDP) must be gained firstly. In this part, the multi-group data obtained in the previous part is regarded as multiple deterministic data groups input to the solution algorithm for obtaining a series of ODDP. In the model, C_u, C_e, C_g and C_{env} are decision variables. Three power balance constraints are used as equality constraints of the model. The inequality constraints of the model include power grid constraint, gas pipeline constraint and equipment constraints. The specific process of this part is demonstrated in Figure 3b.

2.3.1. Objective Function

Considering the minimization of the economic cost and environmental cost of the IES as the optimization objective, the objective formulation can be described as follows:

$$C_{obj} = \min\left\{C_u + C_e + C_g + C_{env}\right\}, \tag{5}$$

where C_u is the cost of all units in the ICES, C_e and C_g are the system cost of power and gas purchase, C_{env} is environmental protection cost which is applied to limit the greenhouse gas emission.

$$C_u = C_{CHP} + u_1 C_{GB} + u_1 C_{EB} + u_2 C_{EC} + u_2 C_{AC} + C_{W,f} + C_{S,f}, \tag{6}$$

Equation (6) shows the cost of all units in the ICES, where C_{CHP} is the cost of CHP units; C_{EB} and C_{GB} are the costs of EB and GB, respectively; C_{EC} and C_{AC} are the costs of EC and AC, respectively; $C_{W,f}$ and $C_{S,f}$ are the cost of WTs and PVs that only consider forecast data, respectively.

$$C_e = \sum_{t=1}^{T} c_e^t P_{buy,e}^t \Delta t, \tag{7}$$

Equation (7) describes the cost of system power purchase, where c_e^t is grid electricity price for each period; $P_{buy,e}^t$ is the power bought from the grid for each period; Δt is the length of time period.

$$C_g = \sum_{t=1}^{T} c_g V_{buy,g}^t, \tag{8}$$

Equation (8) describes the cost of system gas purchase, where c_g is the gas price that is bought from the gas network; $V^t_{buy,g}$ is the amount of gas that is bought from the gas network for each period.

$$C_{env} = \beta \varepsilon_g \sum_{t=1}^{T} \left(V^t_{CHP,g} + V^t_{GB,g} \right), \tag{9}$$

Equation (9) shows the cost of environmental protection, where β is the cost of CO_2 emission for per unit volume; ε_g is the CO_2 emission coefficient for per unit volume of gas; $V^t_{CHP,g}$ and $V^t_{GB,g}$ are the gas consumption of CHP and GB for each period, respectively.

2.3.2. Constraint Condition

- Power balance constraints

According to EH energy coupling matrix, the coupling relationship between input and output power can be obtained. Equations (10)–(12) represent the coupling relationship of ELs, HLs, CLs and GLs, respectively:

$$\begin{cases} P^t_{buy,e} + P^t_{GT,e} + P^t_{W,f,e} + P^t_{S,f,e} = P^t_{L,f,e} + u_1 P^t_{EB,e} + u_2 P^t_{EC,e} \\ u_1 + u_2 = 1 \,\&\, u_1, u_2 \in \{0,1\} \end{cases}, \tag{10}$$

$$\begin{cases} u_1 \left(Q^t_{EB,h} + Q^t_{GT,h} + Q^t_{GB,h} \right) + u_2 \left(Q^t_{EC,c} + Q^t_{AC,c} \right) = u_1 Q^t_{L,h} + u_2 Q^t_{L,c} \\ u_1 + u_2 = 1 \,\&\, u_1, u_2 \in \{0,1\} \end{cases}, \tag{11}$$

$$\begin{cases} V^t_{buy,g} = V^t_{GT,g} + u_1 V^t_{GB,g} + V^t_{L,f,g} \\ u_1 \in \{0,1\} \end{cases}, \tag{12}$$

Specifically, Equation (10) represents electric power balance; Equation (11) represents cooling and heating balance, respectively; Equation (12) describes gas supply and demand balance.

- Network constraints

Network constraints include power network constraint and natural gas network constraints. Specifically, we have:

$$P^{min}_{buy,e} \leqslant P^t_{buy,e} \leqslant P^{max}_{buy,e}, \tag{13}$$

$$V^{min}_{buy,g} \leqslant V^t_{buy,g} \leqslant V^{max}_{buy,g}, \tag{14}$$

where Equation (13) is power grid constraint, Equation (14) is gas pipeline constraint.

- Energy supply equipment and energy coupling equipment constraints

The types of energy supply equipment and energy coupling equipment include PVs, WTs, CHP, GB, EB, AC and EC. The unified constraint model is shown as the following equations.

$$0 \leqslant P^t_m \leqslant P^{max}_m \ (m \in M), \tag{15}$$

$$\begin{cases} \Delta P_m^{min} \leqslant \Delta P_m^t \leqslant \Delta P_m^{max} \\ \Delta P_m^t = P_m^{t+1} - P_m^t \end{cases} (m \in M), \quad (16)$$

where M is the collection of all energy supply equipment and energy coupling devices in the system; P_m^t represents the output value of equipment m in a certain period, and P_m^{max} is the maximum output value of equipment m; ΔP_m^t is the absolute value of the input power variation of energy supply equipment m from period t to (t + 1); ΔP_m^{max} and ΔP_m^{min} are the upper and lower limits of the variation.

2.3.3. Optimization Algorithm

We developed the IPSO algorithm to obtain a series of day-ahead optimal dispatch plans. In the normal PSO, each solution is represented by a group of particles, p_{best} and g_{best}, respectively, represent the personal best solution of particle i and the global best solution among all particles. In order to achieve the optimal solution, the formula for updating velocity v_i and position x_i are described as follows:

$$\begin{cases} v_{id}^{N_{cur}+1} = \omega V_{id}^{N_{cur}} + c_1 r_1 \left(p_{best,id}^{N_{cuc}} - x_{id}^{N_{cur}} \right) + c_2 r_2 \left(g_{best}^{N_{cur}} - x_{id}^{N_{cur}} \right) \\ x_{id}^{N_{cur}+1} = x_{id}^{N_{cur}} + v_{id}^{N_{cur}} \end{cases}, \quad (17)$$

where c_1 and c_2 represent acceleration constants; r_1 and r_2 are random numbers distributed between (0, 1); ω is inertia weight, which is used to balance local exploration and global exploration, inertia weight can be determined by:

$$\omega = \omega_{min} + \left(\omega_{max} - \omega_{min} \right) \frac{N_{cur}}{N}, \quad (18)$$

in the iterative process, the inertia weight obeys a linear evolution, where ω_{max} and ω_{min} are the maximum and minimum values of the inertia weight, respectively. N is the maximum number of iterations and N_{cur} is the current number of iterations.

The normal PSO algorithm has advantages of having fewer parameters and easy implementation. However, it may converge prematurely or fall into a local optimum when handing complex problems such as the optimal dispatch problem discussed in this paper. To solve this problem, the IPSO algorithm is proposed.

The inertia weight factor ω is an important parameter of PSO [33,34], which is applied to control previous velocity influence on the current velocity. Therefore, in the improved algorithm proposed in this paper, the inertia weight ω evolution method in the iterative process is changed. Under the new evolution method, inertia weight is described as follows:

$$\begin{cases} \omega = \omega_{max} - (\omega_{max} - \omega_{min}) \times \left[1 - 2 / (e^{2N_{cur}/N} + 1) \right] \\ rand(N_{cur}) > 0.45 \\ \omega = \omega_{max} - (\omega_{max} - \omega_{min}) \times \left[1 - 2 / (e^{2N_{cur}/N} + 1) \right] \\ rand(N_{cur}) \leqslant 0.45 \end{cases}, \quad (19)$$

where $rand(N_{cur})$ is the random probability of the current iteration number. This strategy makes the adjustment range of ω be gradually compressed and shows a nonlinear decreasing trend as a whole. The addition of probability judgment enhances the randomness of ω under the overall decreasing trend, preventing ω from falling into a monotonous evolution trend, and improving the diversity of particles.

To further prevent the algorithm from easily falling into the local extremum during the iterative process, the best solution perturbation operator (BSPO) is proposed to adjust the personal best solution and the global best solution among all particles. The BSPO updated formula can be determined as follows:

$$\mathrm{BSPO} = d_{max} - \frac{d_{max} - d_{min}}{\mathrm{sum}\left(1:N_{cur}\right)}\left(N - N_{cur}\right), \tag{20}$$

where d_{max} and d_{min} are the maximum and minimum values of the BSPO, respectively. The BSPO decreases nonlinearly as the iteration number increases, which allows particles to perform a large-scale search in early-stage iterations and perform a more precise search in the later stage. The addition of BSPO significantly increases the probability of finding the optimal solution. The updated formula of v_i and x_i after the introduction of BSPO becomes:

$$\begin{cases} v_{id}^{N_{cur}+1} = \omega V_{id}^{N_{cur}} + c_1 r_1 \left(\mathrm{BSOP} \times p_{best,id}^{N_{cur}} - x_{id}^{N_{cur}}\right) + c_2 r_2 \left(\mathrm{BSOP} \times g_{best}^{N_{cur}} - x_{id}^{N_{cur}}\right) \\ x_{id}^{N_{cur}+1} = x_{id}^{N_{cur}} + v_{id}^{N_{cur}} \end{cases}, \tag{21}$$

2.4. Optimal Evolutionary Dispatch Plan (OEDP)

2.4.1. Evolution of Forecast Data

Forecast of renewable energy sources and internal loads can be divided into short-term and long-term ones in line with the leading time scale. Though forecast technologies have been rapidly developing, uncertainties still bring a great challenge for making feasible and beneficial decisions.

The short-term forecasts are more reliable compared with long-term forecasts, but they are limited by forecast horizon which is only several hours. The short-term forecasts are dynamically updated in real time, the forecast data keep evolving and forecast uncertainties would be different as time proceeds. The forecaster releases information for the next a few hours at the current period on the basis of climate information obtained. Hence, the forecast data is not static, evolution existing all the time [35].

2.4.2. Selection and Jointing Strategy of Day-Ahead Deterministic Dispatch Plans

For the optimal dispatch for ICES including renewable energy source, the accuracy of renewable energy source output forecast data can influence the dispatch plan quality significantly.

The applications of long-term forecast give managers and decision makers sufficient time to make proper arrangements for all units in the system, but the long-term forecast data may have a large gap with the actual situation; the dispatch plan made by it always has poor performance. Short-term forecast accuracy is much higher than that of the long-term ones. However, the late announcement time of short-term forecasts makes it not really feasible to dispatch the system.

Hence, a dispatch strategy is proposed to combine the advantages of long-term forecast data and short-term forecast data. Its specific process is as follows:

Selection and Joining Strategy of Day-Ahead Deterministic Dispatch Plans

Step1: Dividing the dispatch period into several equal parts and obtaining short-term forecast data of each part in chronological order.

Step2: The short-term forecast data of each part is compared with series group of long-term forecast data. The long-term forecast data with the highest similarity to the short-term forecast data of each part is selected as best fit data.

Step3: Joining the dispatch plans corresponding to each group of best fit data selected in **Step2** to obtain a complete dispatch plan.

The Euclidean distance is used as a criterion to select the best fit data with the highest similarity to the short-term forecast data of each part. The criterion formula is as follows:

$$\begin{cases} k_i = \min\left\{ED_{ij}\right\} \\ ED_{ij} = \sqrt{\sum_{t=x}^{T}\left(s_i^t - l_j^t\right)^2} \end{cases}, \quad (22)$$

where i and j are group numbers of short-term forecast data and long-term forecast data, respectively; t is time period number and values of x and T depend on the division of the dispatch period; k_i is the group number of the long-term forecast data which has been selected by short-term forecast data i; ED_{ij} is the Euclidean distance between short-term forecast data i and long-term forecast data j; s_i^t and l_j^t are the data of short-term forecast data i and long-term forecast data j, respectively, and both of them are at period t.

The complete dispatch plan obtained through the above strategy can be regarded as a composite scheme established by a series of ODDP. The long-term forecast data is used to derive the day-ahead deterministic dispatch plan, giving managers and decision makers enough time to make reasonable arrangements for the ICES. The short-term forecast data has also been used, which enables the dispatch plan to be able to adapt to the evolution of forecast data in the dispatch process and improve the performance of whole plan. The dispatch plan derived from the strategy proposed in this part is termed as the optimal evolutionary dispatch plan (OEDP).

2.4.3. Real-Time Adjusting Strategy (RAS) for ICES

The strategy proposed in the previous section considers multiple uncertainties and evolution of the forecast data. Nevertheless, there are still some deviations between the data applied in the dispatch plan and the actual situation faced in the dispatch process. In this step, P2G units and energy storage devices, which are not enabled in the previous steps, are turned on to further balance the energy redundancy or shortage caused by the gap between the data and the actual situation. The strategy proposed in this part can be divided into two parts, which are the RAS considering the balance of electric and the RAS considering the balance of natural gas, respectively. The specific process of the strategy is illustrated in Figure 4.

- RAS considering the balance of electric power.

Acquiring the actual data of WTs output ($P_{W,a,e}^t$), PVs output ($P_{S,a,e}^t$) and ELs ($P_{L,a,e}^t$). Subtracting those actual data with the data applied in OEDP ($P_{W,OE,e}^t$, $P_{S,OE,e}^t$ and $P_{L,OE,e}^t$) and obtaining the error of renewable energy sources ($eP_{R,e}^t$) and the error of ELs ($eP_{L,e}^t$). Then, taking the difference between $eP_{R,e}^t$ and $eP_{L,e}^t$ to get the error of electric power (eP_e^t). If eP_e^t is less than zero, the electric energy is redundant. If eP_e^t is greater than zero, power shortage occurs. When eP_e^t is equal to zero, the electric power can maintain the balance state as that in OEDP.

When power redundancy occurs ($eP_e^t < 0$), judging whether the redundant power is less than the capacity of the P2G units ($P_{P2G,e}^{cap}$). If $\left|eP_e^t\right| \le P_{P2G,e}^{cap}$, then all the energy is transferred to the P2G units (Situation 1). Otherwise, judging whether the redundant power is less than the sum of $P_{P2G,e}^{cap}$ and the battery residual capacity ($reP_{B,e}^t$). If

$\left|eP_e^t\right| \le P_{P2G,e}^{cap} + reP_{B,e}^t$, the redundant power that is below $P_{P2G,e}^{cap}$ is transferred to the P2G units, the part in which excess $P_{P2G,e}^{cap}$ is charged into the battery (Situation 2). Otherwise, only if the redundant power exceeds the sum of $P_{P2G,e}^{cap}$ and $reP_{B,e}^t$, energy abandonment phenomenon will occur (Situation 3).

When power shortage occurs ($eP_e^t > 0$), judging whether the shortage part is less than the existing electric power of the battery ($exP_{B,e}^t$). If $eP_e^t \le exP_{B,e}^t$, all the shortage part can be supplied by the battery (Situation 4). Otherwise, purchasing the insufficient part from the power grid (Situation 5).

- RAS considering the balance of natural gas.

Acquiring the actual data of GL ($V_{L,a,g}^t$). Subtracting those actual data with the data applied in OEDP ($V_{L,OE,g}^t$) and obtaining the error of internal GL ($eV_{L,g}^t$). If $eV_{L,g}^t$ is greater than zero, the natural gas is redundant. If $eV_{L,g}^t$ is less than zero, gas shortage occurs. When $eV_{L,g}^t$ is equal to zero, the natural gas can maintain the balance state as in OEDP.

When gas shortage occurs ($eV_{L,g}^t < 0$), first judging whether the shortage part is less than the existing gas volume of the GT ($exV_{GT,g}^t$). If $\left|eV_{L,g}^t\right| \le exV_{GT,g}^t$, then all the shortage part of gas is supplied by the GT (Situation 6). Otherwise, if the shortage part is more than the existing gas volume of the GT, transferring all the gas in gas tank to the community users and the insufficient part is purchased from the gas network (Situation 7).

When gas redundancy occurs ($eV_{L,g}^t > 0$), the gas purchase plan in the OEDP must be reduced immediately (Situation 8).

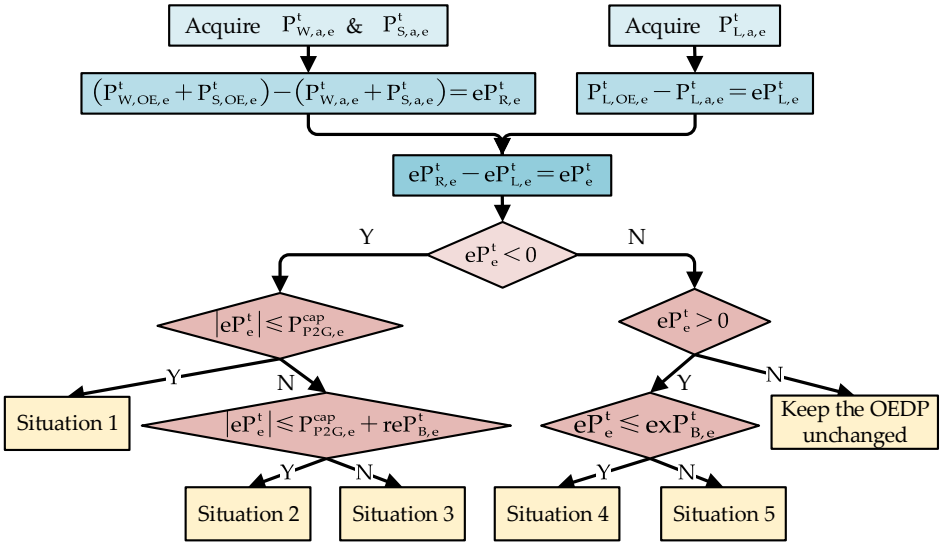

(**a**)

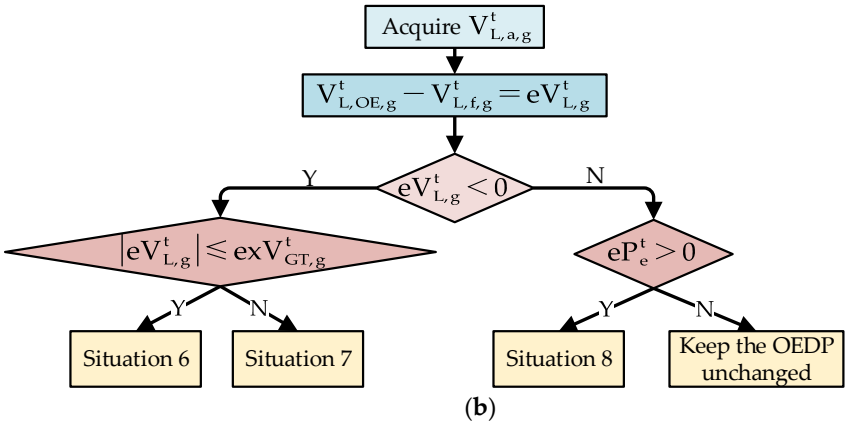

Figure 4. The process of real-time adjusting strategy: (**a**) real-time adjusting strategy considering the balance of electric power; (**b**) real-time adjusting strategy considering the balance of natural gas.

3. Case Study

In this section, a case is presented to verify the superiority of the dispatch method proposed in this article. The ICES model in Figure 2b is used as the basis of this part, and the dispatch method which we need to verify operates on it. A typical day in winter is simulated when the outdoor temperature ranges from −25.2 to −13.6 °C. The gas price of this case is 0.5 USD/m^3, β is set to 10 USD/t and ε_g is set to 2×10^{-3} t/m^3. The electricity price at each period of the day is not constant. The electricity price from 1:00 a.m. to 7:00 a.m. and from 21:00 p.m. to 24:00 p.m. is 7×10^{-2} USD/kWh. The electricity price of 8:00 a.m. and from 13:00 p.m. to 15:00 p.m. is 14×10^{-2} USD/kWh. The electricity price from 9:00 a.m. to 12:00 p.m. and from 16:00 p.m. to 20:00 p.m. is 21×10^{-2} USD/kWh. Table 2 shows the capacity and conversion efficiency of the main units in the ICES. Three subcases are set as follows:

- Subcase 1.

This subcase applies traditional robust optimization method to dispatch. Applying DLFD to get a day-ahead optimal dispatch plan and use it as final operation plan. If there is energy redundancy, the redundant part is directly regarded as abandoned energy; if there is energy shortage, the shortage part is completely purchased from outside.

- Subcase 2.

This subcase applies the MIUS to get a series of ODDP and considering the evolution of SFD to get OEDP. We use OEDP as final operation plan, without introducing RAS. If there is energy redundancy, the redundant part is directly regarded as abandoned energy, if there is energy shortage, the shortage part is completely purchased from outside.

- Subcase 3.

This subcase includes P2G units and energy storage equipment. We introduce MIUS to get a series of ODDP and consider the evolution of SFD to get OEDP. Finally, the RAS is introduced to get the final operation plan.

Among the above subcases, Subcase 3 is completely according to the method proposed in this article, and Subcases 1 and 2 are used for comparison. All simulations are performed on a computer with a 3.40 GHz CPU and 16 GB RAM. The programming is based on the MATLAB R2020a and Yalmip. The MATLAB R2020a is used to solve the programming problem.

Table 2. Capacity and conversion efficiency of the main units.

Equipment	Capacity (MW)	Conversion Efficiency [1]
CHP	85	Power generation: 0.3 Heating: 0.5
GB	80	0.85
EB	70	0.9
EC	100	3.5
AC	100	1.2
P2G	10	0.65

[1] The conversion efficiency represents the efficiency of converting 1 MW electric power into corresponding kinds of energy. There are two examples. Example 1: When 1 MW electric power input EC units, the output of EC units is 3.5 MW cooling power. Example 2: When 1 MW electric power input P2G units, the P2G units can output a certain volume of natural gas containing 0.65 MW power.

3.1. Input Data of Case

A group of test data obtained online is regarded as DLFD [36]. On this basis, we substituted DLFD into MIUS to obtain the multi-group data considering multi-interval uncertainty. We assumed that the forecast error of renewable energy sources and internal loads follow the symmetric normal distribution. The uncertainty set of the deviation ratio was divided into six intervals, i.e., $[-2\sigma, -\sigma]$, $[-\sigma, -0.5\sigma]$, $[-0.5\sigma, 0]$, $[0, 0.5\sigma]$, $[0.5\sigma, \sigma]$, and $[\sigma, 2\sigma]$, where σ is the standard deviation ratio. In the case we proposed, the standard deviation ratio σ was set to 0.1. Except DLFD, other groups of data were divided into two levels according to the degree of uncertainty. Figure 5 shows the data of WTs and ELs to demonstrate the interval division method of MIUS and the multi-group data considering multi-interval uncertainty.

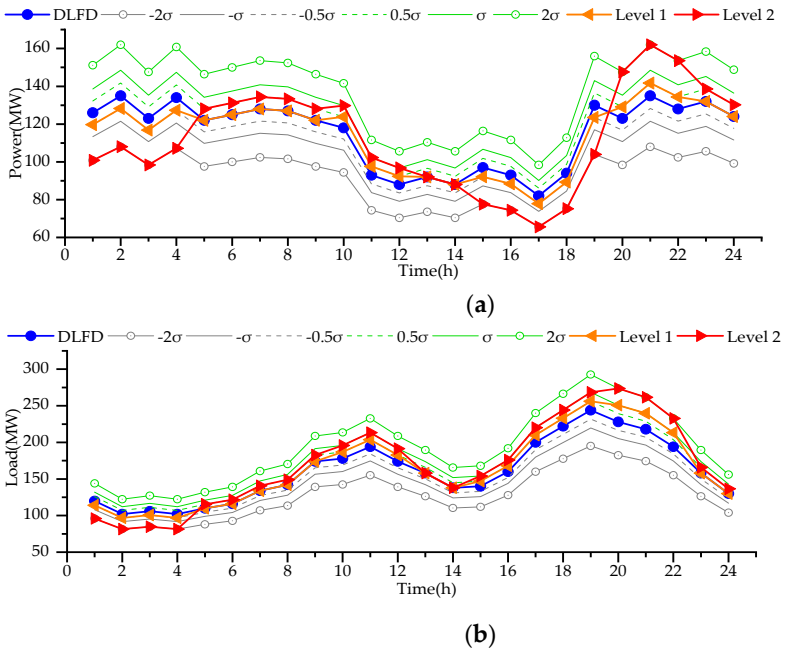

Figure 5. Multi-group data considering multi-interval uncertainty: (**a**) data of WTs; (**b**) data of ELs.

3.2. Dispatch Results of Case

3.2.1. Subcase 1

The DLFD was entered directly into the IPSO to get the ODDP, and the ODDP was used as the final scheduling plan, as shown in Figure 6. Although IPSO can output an ODDP, due to the difference between DLFD and the actual situation of the operating ICES, this subcase will produce vast abandoned energy, it is necessary to frequently adjust the power purchase plan during the peak period of electricity consumption. The economic and environmental benefits of Subcase 1 are not good. The operating cost of ICES in this subcase is USD 6.73×10^5, of which environmental costs account for USD 1.06×10^5.

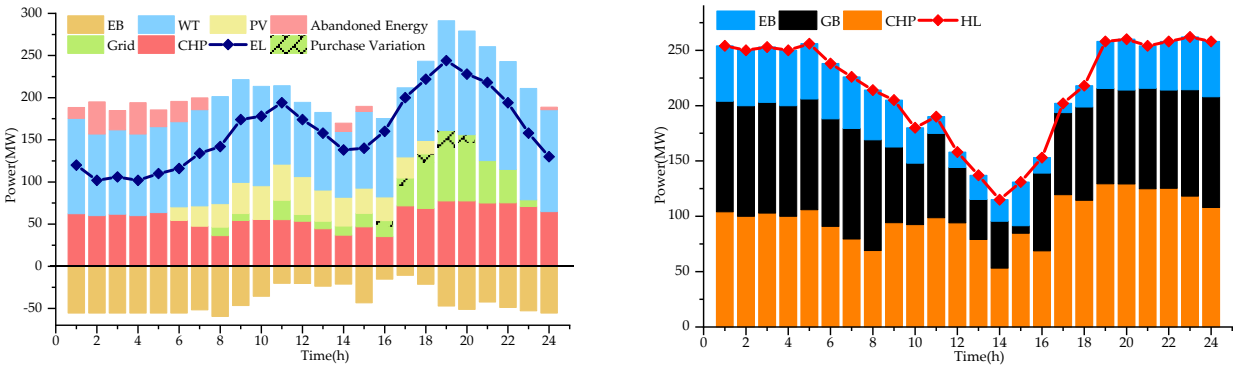

Figure 6. ODDP of Subcase 1: (**a**) dispatch situation of electric power; (**b**) dispatch situation of heating energy.

3.2.2. Subcase 2

We took OEDP as the final operation plan. The uncertainty of renewable energy and internal load was considered, and the evolution of SFD was also considered. The dispatch situation of electric power of Subcase 2 is shown in Figure 7. The dispatch plan in each short-term forecast period is highly matched with the actual situation of the ICES. However, there are also some mild errors in the SFD, and the phenomenon of energy abandonment will still occur. The operating cost of ICES in this subcase is USD 4.57×10^5, of which environmental costs account for USD 8.17×10^4.

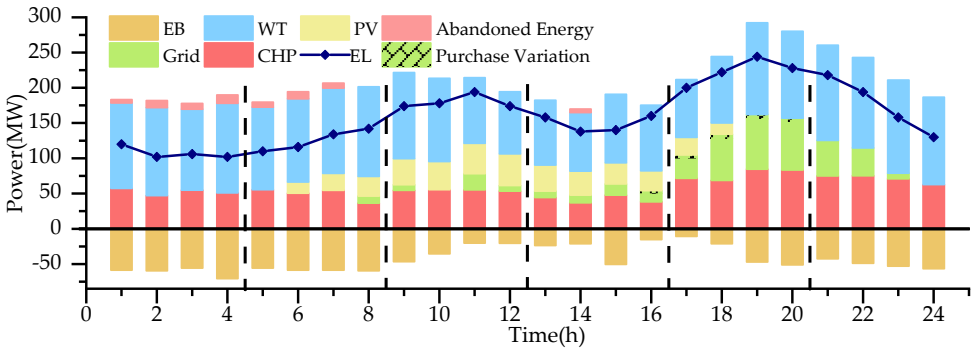

Figure 7. Dispatch situation of electric power of Subcase 2 OEDP.

3.2.3. Subcase 3

OEDP is equivalent to making a dispatch plan for the next four hours based on SFD in four hours advance. Although SFD in four hours advance has high accuracy, there still exist deviations from the actual situation when the system is operating. The RAS is introduced to solve this problem, as shown in the Figure 8.

The introduction of RAS can further absorb the energy that cannot be absorbed in OEDP through P2G units and energy storage equipment. From 1:00 a.m. to 7:00 a.m., P2G units absorbed wind power to avoid energy abandonment. At 16:00 p.m., the actual WT output differs greatly from the SFD, which exceeds the capacity of the P2G units. The excess is charged into the battery, and this part of the electric energy is offered to users when there is a power shortage at 17:00 p.m. The wind energy absorbed by the P2G units is converted into gas for storage and put into utilization when the actual gas demand in the ICE differs from the SFD. Introducing RAS and applying OEDP simultaneously can further improve the economic and environmental benefits of ICES. The operating cost of ICES in this subcase is USD 4.57×10^5, of which environmental costs account for USD 6.26×10^4.

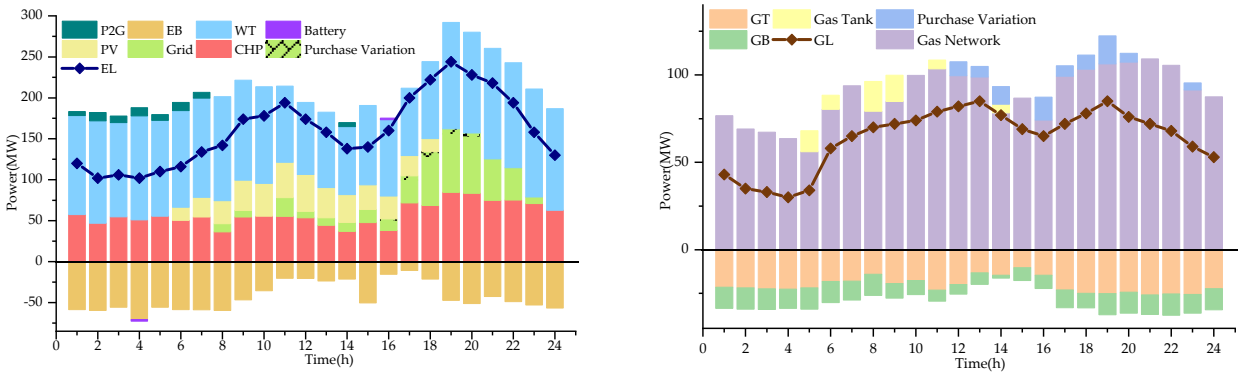

(**a**) (**b**)

Figure 8. Final dispatch plan introducing RAS: (**a**) dispatch situation of electric power; (**b**) dispatch situation of natural gas.

4. Conclusions

In this paper, an evolutionary dispatch method was proposed to solve the energy abandonment problem of ICES under the uncertainties of renewable energy sources and internal loads. Various renewable energy sources and energy conversion units were modeled basing on EH model to improve the flexibility of system. The MIUS was introduced to obtain the multi-group data, which integrated more forecast information than the data only considering single-interval uncertainty. In the whole dispatch process, DLFD is applied to ensure sufficient decision time, and SFD is used to guarantee the performance of the dispatch plan. During the actual operation of the ICES, the renewable energy utilization is further improved through the RAS we proposed.

The proposed method could not only ensure the economic and environmental benefits of the system but also improve the renewable energy utilization. The results of case study illustrated that the uncertainties of renewable energy sources and internal loads have considerable influence on the dispatch results. Compared with the subcase without the method we proposed, the subcase applied in our method has better performance, especially in improving the capacity of renewable energy consumption. However, the application of MIUS will increase the computational time complexity of the model, which also increases a certain amount of calculation cost. Larger computing costs will bring certain challenges to hardware facilities and economic strength, but the increased cost is far less than the benefit brought by the increase in the utilization of renewable energy most of the time. The results of this article indicate that it is necessary to take the uncertainty of renewable energy sources and internal loads into consideration in the dispatch decision of ICES. The achievement obtained in this paper can further improve the renewable energy consumption capacity of ICES and provide a reference for future research on further

improving energy efficiency. Moreover, many other factors, such as random occupant behaviors and district heating system transmission, also have a dramatic impact on system performance, which could be our next topic.

Author Contributions: Conceptualization, X.L. and S.X.; methodology, X.L. and S.X.; software, S.X. and C.G.; validation, X.L., S.X. and C.G.; formal analysis, S.X. and C.G.; investigation, S.X.; resources, S.X. and J.Y.; data curation, S.X. and C.G.; writing—original draft preparation, S.X., G.X., J.Y. and H.C.; writing—review and editing, G.X., J.Y. and H.C.; visualization, G.X. and H.C.; supervision, X.L., J.Y.; project administration, X.L., J.Y. and H.C.; funding acquisition, X.L. and J.Y. All authors have read and agreed to the published version of the manuscript.

Funding: This research was funded by the National Science Foundation of China (under Grant 61903296, U2003110), Innovative Talents Promotion Program-Young Science and Technology Nova Project (2020KJXX-094), Key Laboratory Project of Shaanxi Educational Committee under Grant 20JS110, High Level Talents Plan of Shaanxi Province for Young Professionals, Natural Science Foundation of Shaanxi Province (2021JQ-473), China Postdoctoral Science Foundation (2021M692877).

Institutional Review Board Statement: Not applicable.

Informed Consent Statement: Not applicable.

Data Availability Statement: The data that support the findings of this study are available from the corresponding author upon reasonable request.

Conflicts of Interest: The authors declare no conflict of interest.

References

1. Correa-Posada, C.M.; Sanchez-Martin, P. Integrated Power and Natural Gas Model for Energy Adequacy in Short-Term Operation. *IEEE Trans. Power Syst.* **2015**, *30*, 3347–3355, doi:10.1109/tpwrs.2014.2372013.
2. Hassan, H.A.H.; Pelov, A.; Nuaymi, L. Integrating Cellular Networks, Smart Grid, and Renewable Energy: Analysis, Architecture, and Challenges. *IEEE Access* **2015**, *3*, 2755–2770, doi:10.1109/access.2015.2507781.
3. Figaj, R.; Żołądek, M. Operation and Performance Assessment of a Hybrid Solar Heating and Cooling System for Different Configurations and Climatic Conditions. *Energies* **2021**, *14*, 1142, doi:10.3390/en14041142.
4. Xu, X.; Jin, X.; Jia, H.; Yu, X.; Li, K. Hierarchical management for integrated community energy systems. *Appl. Energy* **2015**, *160*, 231–243, doi:10.1016/j.apenergy.2015.08.134.
5. Miao, B.; Lin, J.; Li, H.; Liu, C.; Li, B.; Zhu, X.; Yang, J. Day-Ahead Energy Trading Strategy of Regional Integrated Energy System Considering Energy Cascade Utilization. *IEEE Access* **2020**, *8*, 138021–138035, doi:10.1109/access.2020.3007224.
6. Boutsika, T.; Santoso, S. Quantifying Short-Term Wind Power Variability Using the Conditional Range Metric. *IEEE Trans. Sustain. Energy* **2012**, *3*, 369–378, doi:10.1109/tste.2012.2186617.
7. Zhong, W.; Chen, J.; Liu, M.; Murad, M.; Milano, F. Coordinated Control of Virtual Power Plants to Improve Power System Short-Term Dynamics. *Energies* **2021**, *14*, 1182, doi:10.3390/en14041182.
8. Aboobacker, V.; Shanas, P.; Veerasingam, S.; Al-Ansari, E.; Sadooni, F.; Vethamony, P. Long-Term Assessment of Onshore and Offshore Wind Energy Potentials of Qatar. *Energies* **2021**, *14*, 1178, doi:10.3390/en14041178.
9. Vallejo, D.; Cornalino, E.; Chaer, R. Genetic algorithm applied to the specialization of neural networks for the forecast of wind and solar generation. In Proceedings of the 2018 IEEE 9th Power, Instrumentation and Measurement Meeting (EPIM), Salto, Uruguay, 14–18 November 2018; pp. 1–4, doi:10.1109/epim.2018.8756397.
10. Alrashidi, M.; Alrashidi, M.; Pipattanasomporn, M.; Rahman, S. Short-term PV output forecasts with support vector regression optimized by cuckoo search and differential evolution algorithms. In Proceedings of the 2018 IEEE International Smart Cities Conference (ISC2), Kansas City, MO, USA, 16–19 September 2018.
11. Makhloufi, S.; Debbache, M.; Boulahchiche, S. Long-term forecasting of intermittent wind and photovoltaic resources by using Adaptive Neuro Fuzzy Inference System (ANFIS). In Proceedings of the 2018 International Conference on Wind Energy and Applications in Algeria (ICWEAA), Algiers, Algeria, 6–7 November 2018; pp. 1–4.
12. Hosseini, S.M.; Carli, R.; Dotoli, M. A residential demand-side management strategy under nonlinear pricing based on robust model predictive control. In Proceedings of the 2019 IEEE International Conference on Systems, Man and Cybernetics (SMC), Bari, Italy, 6–9 October 2019; pp. 3243–3248.
13. Giraldo, J.S.; Castrillon, J.A.; Lopez, J.C.; Rider, M.J.; Castro, C.A. Microgrids Energy Management Using Robust Convex Programming. *IEEE Trans. Smart Grid* **2018**, *10*, 4520–4530, doi:10.1109/tsg.2018.2863049.
14. Yang, L.; Zhang, X.; Gao, P. Research on heat and electricity coordinated dispatch model for better integration of wind power based on electric boiler with thermal storage. *IET Gener. Transm. Distrib.* **2018**, *12*, 3736–3743, doi:10.1049/iet-gtd.2017.2032.
15. Liu, B.; Li, J.; Zhang, S.; Gao, M.; Ma, H.; Li, G.; Gu, C. Economic Dispatch of Combined Heat and Power Energy Systems Using Electric Boiler to Accommodate Wind Power. *IEEE Access* **2020**, *8*, 41288–41297, doi:10.1109/access.2020.2968583.

16. Révész, Á.; Gajdics, M. High-Pressure Torsion of Non-Equilibrium Hydrogen Storage Materials: A Review. *Energies* **2021**, *14*, 819, doi:10.3390/en14040819.
17. Lu, S.; Gu, W.; Zhou, S.; Yao, S.; Pan, G. Adaptive Robust Dispatch of Integrated Energy System Considering Uncertainties of Electricity and Outdoor Temperature. *IEEE Trans. Ind. Inform.* **2020**, *16*, 4691–4702, doi:10.1109/tii.2019.2957026.
18. Lu, S.; Gu, W.; Meng, K.; Dong, Z.Y. Economic Dispatch of Integrated Energy Systems with Robust Thermal Comfort Management. *IEEE Trans. Sustain. Energy* **2021**, *12*, 222–233, doi:10.1109/tste.2020.2989793.
19. Yu, J.; Shen, X.; Sun, H. Economic Dispatch for Regional Integrated Energy System with District Heating Network Under Stochastic Demand. *IEEE Access* **2019**, *7*, 46659–46667, doi:10.1109/access.2019.2905772.
20. Tor, O.B.; Shahidehpour, M. Crossroads of Power: Coordinating Electricity and Natural Gas Infrastructures in Turkey. *IEEE Power Energy Mag.* **2014**, *12*, 49–62, doi:10.1109/mpe.2014.2347653.
21. Qiu, J.; Dong, Z.Y.; Zhao, J.H.; Meng, K.; Zheng, Y.; Hill, D.J. Low Carbon Oriented Expansion Planning of Integrated Gas and Power Systems. *IEEE Trans. Power Syst.* **2014**, *30*, 1035–1046, doi:10.1109/tpwrs.2014.2369011.
22. Clegg, S.; Mancarella, P. Integrated Modeling and Assessment of the Operational Impact of Power-to-Gas (P2G) on Electrical and Gas Transmission Networks. *IEEE Trans. Sustain. Energy* **2015**, *6*, 1234–1244, doi:10.1109/tste.2015.2424885.
23. Geidl, M.; Koeppel, G.; Favre-Perrod, P.; Klockl, B.; Andersson, G.; Frohlich, K. Energy hubs for the future. *IEEE Power Energy Mag.* **2007**, *5*, 24–30, doi:10.1109/mpae.2007.264850.
24. Rayati, M.; Sheikhi, A.; Ranjbar, A.M. Applying reinforcement learning method to optimize an Energy Hub operation in the smart grid. In Proceedings of the 2015 IEEE Power & Energy Society Innovative Smart Grid Technologies Conference (ISGT), Washington, DC, USA, 18–20 February 2015; pp. 1–5.
25. Skov, I.; Schneider, N.; Schweiger, G.; Schöggl, J.-P.; Posch, A. Power-to-X in Denmark: An Analysis of Strengths, Weaknesses, Opportunities and Threats. *Energies* **2021**, *14*, 913, doi:10.3390/en14040913.
26. Zhou, L.; Liu, N.; Zhang, Y. Energy management for smart energy hub considering gas dispatch factor and demand response. In Proceedings of the 2018 2nd IEEE Conference on Energy Internet and Energy System Integration (EI2), Beijing, China, 20–22 October 2018; pp. 1–6.
27. Daneshvar, M.; Mohammadi-Ivatloo, B.; Asadi, S.; Zare, K.; Anvari-Moghaddam, A. Optimal day-ahead scheduling of the renewable based energy hubs considering demand side energy management. In Proceedings of the 2019 International Conference on Smart Energy Systems and Technologies (SEST), Porto, Portugal, 9–11 September 2019; pp. 1–6.
28. Lu, S.; Gu, W.; Zhou, S.; Yu, W.; Yao, S.; Pan, G. High-Resolution Modeling and Decentralized Dispatch of Heat and Electricity Integrated Energy System. *IEEE Trans. Sustain. Energy* **2019**, *11*, 1451–1463, doi:10.1109/tste.2019.2927637.
29. Shao, C.; Ding, Y.; Wang, J.; Song, Y. Modeling and Integration of Flexible Demand in Heat and Electricity Integrated Energy System. *IEEE Trans. Sustain. Energy* **2018**, *9*, 361–370, doi:10.1109/tste.2017.2731786.
30. Zhang, C.; Xu, Y.; Dong, Z.Y.; Ma, J. Robust Operation of Microgrids via Two-Stage Coordinated Energy Storage and Direct Load Control. *IEEE Trans. Power Syst.* **2017**, *32*, 2858–2868, doi:10.1109/tpwrs.2016.2627583.
31. Bertsimas, D.; Litvinov, E.; Sun, X.A.; Zhao, J.; Zheng, T. Adaptive Robust Optimization for the Security Constrained Unit Commitment Problem. *IEEE Trans. Power Syst.* **2013**, *28*, 52–63, doi:10.1109/tpwrs.2012.2205021.
32. Qiu, H.; Gu, W.; Xu, Y.; Wu, Z.; Zhou, S.; Wang, J. Interval-Partitioned Uncertainty Constrained Robust Dispatch for AC/DC Hybrid Microgrids With Uncontrollable Renewable Generators. *IEEE Trans. Smart Grid* **2018**, *10*, 4603–4614, doi:10.1109/tsg.2018.2865621.
33. Ravan, M.; Amineh, R.K.; Koziel, S.; Nikolova, N.K.; Reilly, J.P. Sizing of 3-D Arbitrary Defects Using Magnetic Flux Leakage Measurements. *IEEE Trans. Magn.* **2009**, *46*, 1024–1033, doi:10.1109/tmag.2009.2037008.
34. Kahouli, O.; Alsaif, H.; Bouteraa, Y.; Ben Ali, N.; Chaabene, M. Power System Reconfiguration in Distribution Network for Improving Reliability Using Genetic Algorithm and Particle Swarm Optimization. *Appl. Sci.* **2021**, *11*, 3092, doi:10.3390/app11073092.
35. Yang, Z.; Yang, K.; Wang, Y.; Su, L.; Hu, H. Multi-objective short-term hydropower generation operation for cascade reservoirs and stochastic decision making under multiple uncertainties. *J. Clean. Prod.* **2020**, *276*, 122995, doi:10.1016/j.jclepro.2020.122995.
36. Test Data for Small IES. Available online: https://www.dropbox.com/s/2yxa37pstuyxy38/Data_ARDM_Small_IES.xlsx?dl=0 (accessed on 14 February 2021).